Dynamics of the Wigner crystal of composite particles

Junren Shi[1,2,*] and Wencheng Ji[1]
[1]*International Center for Quantum Materials, Peking University, Beijing 100871, China*
[2]*Collaborative Innovation Center of Quantum Matter, Beijing 100871, China*

(Received 13 April 2017; revised manuscript received 14 February 2018; published 20 March 2018)

Conventional wisdom has long held that a composite particle behaves just like an ordinary Newtonian particle. In this paper, we derive the effective dynamics of a type-I Wigner crystal of composite particles directly from its microscopic wave function. It indicates that the composite particles are subjected to a Berry curvature in the momentum space as well as an emergent dissipationless viscosity. While the dissipationless viscosity is the Chern-Simons field counterpart for the Wigner crystal, the Berry curvature is a feature not presented in the conventional composite fermion theory. Hence, contrary to general belief, composite particles follow the more general Sundaram-Niu dynamics instead of the ordinary Newtonian one. We show that the presence of the Berry curvature is an inevitable feature for a dynamics conforming to the dipole picture of composite particles and Kohn's theorem. Based on the dynamics, we determine the dispersions of magnetophonon excitations numerically. We find an emergent magnetoroton mode which signifies the composite-particle nature of the Wigner crystal. It occurs at frequencies much lower than the magnetic cyclotron frequency and has a vanishing oscillator strength in the long-wavelength limit.

DOI: 10.1103/PhysRevB.97.125133

I. INTRODUCTION

In a two-dimensional electron gas (2DEG) subjected to a strong magnetic field, electrons are forced into Landau levels with the kinetic energy quenched. The dominating electron-electron interaction induces various correlated ground states. The most celebrated of these states is the fractional quantum Hall (FQH) liquid which occurs in the vicinity of a set of magnetic filling factors of rational fractions [1]. Interestingly, even though the system is dominated by the electron-electron interaction, its physics can be well described in a hidden Hilbert space by a set of weakly interacting composite fermions (bosons) that are bound states of an electron with an even (odd) number of quantum vortices, as suggested by the theory of composite fermions (CFs) [1,2]. In the theory, a FQH state is interpreted as an integer quantum Hall state of CFs. The theory achieves great successes. For instance, ground-state wave functions prescribed by the CF theory for the FQH states achieve high overlaps with those determined from exact diagonalizations [1], and predictions based on an intuitive picture of noninteracting CFs are verified in various experiments [3]. The theory can even be applied to more exotic situations such as the half-filling case which is interpreted as a Fermi liquid of CFs [4,5], and the 5/2-filling case which is interpreted as a p-wave pairing state of CFs [6]. In effect, for every known state of electrons, one could envision a counterpart for CFs.

It is natural to envision that CFs may form a Wigner crystal (WC). Electrons form a Wigner crystal at sufficiently low density when the Coulomb interaction between electrons dominates over the kinetic energy [7]. In the presence of a strong external magnetic field, the kinetic energy is completely quenched and electrons should have a tendency to form a crystalline phase. However, in a 2DEG, the tendency is preempted by the more stable FQH states when the filling factor is close to special fractions such as 1/3 and 2/5. Nevertheless, a WC could be stabilized when the filling factor deviates from these fractions. Theoretical studies suggest that the WC of composite particles (CPWC), i.e., a WC consisting not of electrons but of composite fermions or bosons, could be stabilized [8]. More specifically, either a type-I CPWC [8,9], in which all composite particles (CPs) are frozen, or a type-II CPWC [10], which lives on top of a FQH state and only freezes CFs excessive for the filling fraction of the FQH state, could be energetically favored over the ordinary electron WC [8,11–15]. Experimentally, there has accumulated a large number of evidences indicating the formation of WCs in 2DEG systems, although these experiments, either detecting the microwave resonances of disorder pinning modes [16–24] or measuring transport behaviors [24–31], cannot unambiguously distinguish a CPWC from its ordinary electron counterpart.

A possible way to distinguish a CPWC from its ordinary electron counterpart is to examine its low-energy phonon excitation. The phonon excitation of an ordinary WC has been thoroughly investigated [32–34]. It consists of a low-frequency branch and a magnetoplasmon mode that occurs near the magnetic cyclotron frequency. For a CPWC, in analog to the ordinary WC, one would expect that its phonon excitation also consists of two branches. However, similar to the magnetoroton mode arisen in FQH liquids [35], its high-frequency branch must be an emergent mode originated purely from the electron-electron interaction, irrelevant to the cyclotron resonance because all excitations of CPs are limited within a partially filled Landau level. Moreover, Kohn's theorem asserts that the ordinary magnetic cyclotron mode exhausts all the spectral weight in the long-wavelength limit [4,36]. To be

*junrenshi@pku.edu.cn

consistent with Kohn's theorem, the emergent mode must have a vanishing oscillator strength in the long-wavelength limit. These features of the emergent mode make it distinguishable from the ordinary magnetoplasmon mode. An experimental probe of the mode would provide an unambiguous evidence for the CP nature of an observed WC phase.

To determine the low-energy phonon excitation of a CPWC, it is necessary to understand the dynamics of CPs. Unfortunately, up to now, the true nature of the CP dynamics is yet to be fully clarified. Existing theories are based on a heuristic approach assuming that CPs follow the ordinary dynamics characterized by an effective mass and an effective magnetic field [37–39]. The assumption is in accordance with the conventional wisdom that a CP behaves just like an ordinary Newtonian particle, as implied in either the Halperin-Lee-Read theory of composite Fermi liquids [5] or López-Fradkin's construction of the Chern-Simons field theory for FQH states [40]. However, the validity of the assumption is questionable. An indication of that is the violation of Kohn's theorem: the heuristic approach would predict a new cyclotron mode corresponding to the effective mass and magnetic field. More fundamentally, there is no *a priori* reason to believe that CPs would follow the ordinary Newtonian dynamics in its simplest form. Actually, even for electrons in a solid, the dynamics in general has a symplectic form (Sundaram-Niu dynamics) with Berry curvature corrections [41,42], and for a magnetic solid its lattice dynamics is in general subjected to a dissipationless viscosity which is the counterpart of the Lorentz force for the atom-atom interaction [43,44]. Recently, Son also questions the validity of the assumption by noting inconsistencies in the conventional Halperin-Lee-Read theory of CF Fermi liquids, and hypothesizes that a CF would be a massless Dirac particle [45,46]. We note that the dynamics of massless Dirac particles is subjected to a Berry curvature in the momentum space with a singular distribution.

We believe that a concrete answer to the question should be a derivation of the CP dynamics directly from microscopic wave functions. The theory of CFs, as detailed in Ref. [1], is not only an intuitive picture for describing FQH states but also a systematic way for constructing ground-state wave functions as well as the Hilbert space of low-lying excitations. This information is sufficient for an unambiguous determination of the dynamics. Conversely, a proposal on the nature of CFs should have an implication on how the microscopic states would be constructed. Unfortunately, the correspondence between the microscopic states and the dynamics is rarely explicitly demonstrated in literatures. A rare example of the correspondence can be found in the dipole picture of CFs [47], which is based on the microscopic Rezayi-Read wave function for a CF Fermi liquid [48]. However, even in this case, an explicit form of the dynamics has never been properly formulated (see Sec. III B).

In this paper, we derive the effective dynamics of CPs directly from the microscopic wave function of the CPWC. The derivation is based on the time-dependent variational principle [49]. We focus on the type-I CPWC, which is relatively simple without unnecessarily obscuring complexities. Based on the dynamics, we conclude that a CP, at least in the CPWC phase, is neither an ordinary Newtonian particle nor a Dirac particle, but a particle subjected to a Berry curvature uniformly distributed in the momentum space as well as an emergent dissipationless viscosity [43,44], and follows the more general Sundaram-Niu dynamics. We carry out numerical simulations to quantitatively determine the dispersions of phonons. We find an emergent magnetoroton mode which signifies the CP nature of a WC. The mode occurs at frequencies much lower than the magnetic cyclotron frequency, and has a vanishing oscillator strength in the long-wavelength limit, consistent with Kohn's theorem.

The most notable feature of the dynamics is the presence of a Berry curvature in the momentum space. This is a feature not presented in the conventional CF theory. It is a direct consequence of the microscopic wave function we adopt for the CPWC, instead of a result of *ad hoc* assumptions. The presence of the Berry curvature is not only necessary for correct quantitative calculations of the low-lying excitations, but also inevitable if one would like to have a dynamics conforming to the dipole picture of CFs as well as Kohn's theorem, as shown in Sec. III B. While the correction looks like a minor one, it is actually sufficient to cure some long-standing issues of the conventional CF theory [50]. We thus argue that the Berry curvature would be an indispensable component of a proper theory of the CP dynamics.

The remainder of the paper is organized as follows. In Sec. II, we derive the CP dynamics from the microscopic wave function of the CPWC phase. In Sec. III, we discuss CP pictures emerged from the dynamics. In Sec. IV, we carry out the numerical simulations based on the formalism, and present quantitative results for the dispersions of the phonon excitations. Finally, Sec. V contains concluding remarks.

II. CP DYNAMICS IN A CPWC

A. CPWC wave function

The theory of CFs prescribes an ansatz for constructing the wave functions of the ground-state and low-lying excited states of a CF system. A CF wave function is derived from a Hartree-Fock wave function $\Psi_{\rm HF}$, which describes the quantum state of a collection of weakly interacting particles in a fictitious (hidden) Hilbert space. The CF wave function is obtained by a transformation from $\Psi_{\rm HF}$ [1,2]:

$$\Psi(\{\boldsymbol{r}_i\}) = \hat{P}_{\rm LLL} J \Psi_{\rm HF}(\{\boldsymbol{r}_i\}), \tag{1}$$

where $\hat{P}_{\rm LLL}$ denotes the projection to the lowest Landau level (LLL), and

$$J = \prod_{i<j} (z_i - z_j)^m \tag{2}$$

is the Bijl-Jastrow factor which binds an integer number of m quantum vortices to each of the electrons, $z_i = x_i + i y_i$ with $\boldsymbol{r}_i \equiv (x_i, y_i)$ being the coordinate of an electron [51]. Equation (1) maps a state in the conventional Landau-Fermi paradigm to a CF state. Using different Landau-Fermi states and following the ansatz, it is possible to construct a whole array of CF wave functions corresponding to various states observed in 2DEGs. For instance, a set of filled Landau levels is mapped to a FQH state [1], a Fermi liquid is mapped to a CF Fermi liquid [4,5], and a p-wave superconductor is mapped to the Moore-Read state [6].

For the ground state of a type-I CPWC, $\Psi_{\rm HF}$ is chosen to be [8]

$$\Psi_{\rm HF}(\{\boldsymbol{r}_i\}) = \hat{\mathcal{A}} \prod_i \phi_{\boldsymbol{R}_i^0}(\boldsymbol{r}_i), \tag{3}$$

where $\phi_{\boldsymbol{R}_i^0}(\boldsymbol{r}_i) \propto \exp[-(\boldsymbol{r}_i - \boldsymbol{R}_i^0)^2/4l_B^2 - i(\hat{z}\times\boldsymbol{r}_i)\cdot\boldsymbol{R}_i^0/2l_B^2]$ is the wave function of a LLL coherent state centering at $\boldsymbol{R}_i^0$ [32], $\{\boldsymbol{R}_i^0, i = 1\ldots N\}$ forms a two-dimensional triangular lattice, $\hat{\mathcal{A}}$ denotes the (anti-) symmetrization of the wave function, and $l_B \equiv \sqrt{\hbar/eB}$ is the magnetic length for the external magnetic field B. We note that $\Psi_{\rm HF}$ is actually the trial wave function for an ordinary electron WC in the LLL [32]. The mapping of Eq. (1) transforms it to a trial wave function for the CPWC with a variational parameter m. Different from usual CF wave functions, m for a CPWC wave function can be even (CF) or odd (composite boson). This is because electrons in a CPWC are spatially localized and not sensitive to the exchange symmetry. Extensive numerical simulations based on the trial wave function have been carried out in Ref. [8]. It was shown that a type-I CPWC is indeed energetically favored over the ordinary electron WC.

The low-lying excited states can be constructed by modifying $\Psi_{\rm HF}$. An apparent modification is to replace $\{\boldsymbol{R}_i^0\}$ with $\{\boldsymbol{R}_i \equiv \boldsymbol{R}_i^0 + \boldsymbol{u}_i\}$ which introduces deviations of the particles from their equilibrium positions. Another physically motivated modification is to introduce a momentum for each particle. This can be achieved by replacing $\phi_{\boldsymbol{R}}(\boldsymbol{r})$ with $\phi_{\boldsymbol{R}}(\boldsymbol{r})\exp(i\boldsymbol{k}\cdot\boldsymbol{r})$, as apparent for a localized wave packet with a momentum $\boldsymbol{p} = \hbar\boldsymbol{k}$. We note that the similar approach is also adopted in constructing Rezayi-Read's wave function for a CF Fermi liquid as well as its particle-hole excitations [48], and in Girvin-MacDonald-Platzman theory of magnetorotons in FQH liquids [35]. The modifications result in a wave function parameterized in $\{\boldsymbol{R}_i\}$ and $\{\boldsymbol{k}_i\}$:

$$\Psi(\{\boldsymbol{r}_i\}) \propto \mathcal{A}\hat{P}_{\rm LLL}\prod_{i<j}(z_i - z_j)^m \prod_i \phi_{\boldsymbol{R}_i}(\boldsymbol{r}_i)e^{i\boldsymbol{k}_i\cdot\boldsymbol{r}_i}, \tag{4}$$

which specifies a submanifold in the Hilbert space. We assume that the ground-state and low-lying phononic excited states of a CPWC completely lie in the submanifold.

Following the standard procedure of applying the projection to the LLL [1], we obtain the explicit form of the wave function (4):

$$\Psi(\{\boldsymbol{r}_i\}) \propto \mathcal{A}\prod_{i<j}\left(z_i + ik_i l_B^2 - z_j - ik_j l_B^2\right)^m \prod_i \phi_{\boldsymbol{R}_i}(\boldsymbol{r}_i), \tag{5}$$

where $k_i \equiv k_{xi} + ik_{yi}$, and we have made a substitution $\boldsymbol{R}_i + \boldsymbol{k}_i l_B^2 \times \hat{z} \to \boldsymbol{R}_i$, and dropped irrelevant normalization and phase factors. We will base our derivation of the CP dynamics on the ansatz wave function Eq. (5).

The physical meaning of the momentum $\hbar\boldsymbol{k}_i$ becomes apparent in Eq. (5). It shifts z_i in the Bijl-Jastrow factor to $z_i^v \equiv z_i + ik_i l_B^2$. One could interpret z_i^v as the position of quantum vortices binding with the ith electron. The momentum is actually the spatial separation of the electron and the quantum vortices in a CP. This is exactly the interpretation of the dipole picture of CFs proposed by Read [47]. We note that the momentum degrees of freedom are only present in systems with $m \neq 0$. For an ordinary WC with $m = 0$, the momenta have no effect on the wave function except introducing a reparametrization to $\{\boldsymbol{R}_i\}$. Therefore, the momenta are emergent degrees of freedom of a CP system.

When adopting the ansatz wave function Eq. (5), we basically assume that the CPWC state belongs to the same paradigm as that for FQH states. Viewed from the new CF paradigm, the modifications introduced in Eq. (5) are well motivated in physics, notwithstanding its highly nontrivial form. The paradigm of CFs, which dictates how the ground-state and low-lying excited states are constructed, has been extensively tested in literatures for various FQH states [1]. It is reasonable to believe that the CPWC also fits in with the paradigm. This can be tested by comparing the wave functions generated by the ansatz with those obtained by diagonalizing microscopic Hamiltonians. In this paper, we will not carry out the test. Instead, we will focus on an immediate question; i.e., if one adopted the paradigm *per se*, what would be the dynamics?

It can also be shown that our ansatz wave-function approach is equivalent to a CF diagonalization [1] (see Secs. II C and II D). The equivalence could serve as a justification for our approach. Our approach is advantageous in the sense that it provides direct knowledge of the dynamics of CPs, whereas the CF diagonalization technique provides an efficient machinery for systematically improving calculations but little information about the dynamics.

B. Derivation of the CP dynamics

To determine the dynamics of CPs in a CPWC, we employ the time-dependent variational principle of quantum mechanics. It minimizes an action $S \equiv \int_{t_i}^{t_f} L dt$ with the Lagrangian [49]:

$$L = \frac{i\hbar}{2}\frac{\langle\Psi|\dot{\Psi}\rangle - \langle\dot{\Psi}|\Psi\rangle}{\langle\Psi|\Psi\rangle} - V_{ee}, \tag{6}$$

where we assume that the wave function depends on the time through its parameters $\{\boldsymbol{R}_i, \boldsymbol{k}_i\}$, $V_{ee} \equiv \langle\Psi|\hat{V}_{ee}|\Psi\rangle/\langle\Psi|\Psi\rangle$ is the expectation value of the electron-electron interaction $\hat{V}_{ee}$, and the kinetic part of the microscopic Hamiltonian of the system is ignored since it is quenched in the LLL. A minimization of the action will result in a set of semiclassical equations of motion [41]. Alternatively, one could interpret the action as the one determining the path-integral amplitude of a quantum evolution in the submanifold of the Hilbert space [52]. The two interpretations are corresponding to the classical and quantum version of the same dynamics, respectively.

We proceed to determine the explicit form of the Lagrangian. The Lagrangian can be expanded as

$$L = \sum_i (\boldsymbol{A}_{\boldsymbol{u}_i}\cdot\dot{\boldsymbol{u}}_i + \boldsymbol{A}_{\boldsymbol{k}_i}\cdot\dot{\boldsymbol{k}}_i) - V_{ee}, \tag{7}$$

where $\boldsymbol{A}_{\boldsymbol{u}_i}$ and $\boldsymbol{A}_{\boldsymbol{k}_i}$ are Berry connections in the parameter space, $\boldsymbol{A}_{\boldsymbol{u}_i} = -\hbar{\rm Im}\langle\Psi|\partial\Psi/\partial\boldsymbol{u}_i\rangle/\langle\Psi|\Psi\rangle$ and $\boldsymbol{A}_{\boldsymbol{k}_i} = -\hbar{\rm Im}\langle\Psi|\partial\Psi/\partial\boldsymbol{k}_i\rangle/\langle\Psi|\Psi\rangle$, respectively. By using Eq. (5), it is straightforward to obtain

$$\boldsymbol{A}_{\boldsymbol{u}_i} = -\frac{\hbar}{2l_B^2}\langle\hat{\boldsymbol{r}}_i\rangle\times\hat{z}, \tag{8}$$

$$\boldsymbol{A}_{\boldsymbol{k}_i} = -m\hbar l_B^2\left\langle\sum_{j\neq i}\frac{\boldsymbol{r}_i - \boldsymbol{r}_j + \hat{z}\times(\boldsymbol{k}_i - \boldsymbol{k}_j)l_B^2}{\left|\boldsymbol{r}_i - \boldsymbol{r}_j + \hat{z}\times(\boldsymbol{k}_i - \boldsymbol{k}_j)l_B^2\right|^2}\right\rangle, \tag{9}$$

where $\langle \dots \rangle \equiv \langle \Psi | \dots | \Psi \rangle / \langle \Psi | \Psi \rangle$, and we ignore the antisymmetrization in the wave function Eq. (4). The antisymmetrization can be reimposed when formulating the quantum version of the dynamics by introducing an antisymmetrization with respect to the parameters (dynamic variables). For CPWCs, the effect due to the nondistinguishability of electrons turns out to be negligible [8].

The Berry connections could be simplified. We make use of the identity

$$\nabla_{\boldsymbol{r}_i}|\Psi|^2 = -\frac{\boldsymbol{r}_i - \boldsymbol{R}_i}{l_B^2}|\Psi|^2 + 2m\sum_{j\neq i}\frac{\boldsymbol{r}_i - \boldsymbol{r}_j + \hat{z}\times(\boldsymbol{k}_i - \boldsymbol{k}_j)l_B^2}{\left|\boldsymbol{r}_i - \boldsymbol{r}_j + \hat{z}\times(\boldsymbol{k}_i - \boldsymbol{k}_j)l_B^2\right|^2}|\Psi|^2. \tag{10}$$

Substituting Eq. (10) into Eq. (9), we obtain

$$\boldsymbol{A}_{\boldsymbol{k}_i} = -\frac{\hbar}{2}(\langle\hat{\boldsymbol{\xi}}_i\rangle - \boldsymbol{u}_i), \tag{11}$$

where $\hat{\boldsymbol{\xi}}_i \equiv \hat{\boldsymbol{r}}_i - \boldsymbol{R}_i^0$. The Berry connections can then be expressed as

$$\boldsymbol{A}_{\boldsymbol{u}_i} = -\frac{\hbar}{2l_B^2}\boldsymbol{x}_i\times\hat{z} + \frac{\hbar\boldsymbol{k}_i}{2}, \tag{12}$$

$$\boldsymbol{A}_{\boldsymbol{k}_i} = -\frac{\hbar}{2}\left(\boldsymbol{x}_i - \boldsymbol{u}_i + \boldsymbol{k}_i\times\hat{z}l_B^2\right), \tag{13}$$

where $\boldsymbol{x}_i \equiv \langle\hat{\boldsymbol{\xi}}_i\rangle - \boldsymbol{k}_i\times\hat{z}l_B^2$, $\hat{z}$ is the unit normal vector of the 2DEG plane. We note that $\boldsymbol{x}_i$ is the average position (relative to $\boldsymbol{R}_i^0$ [53]) of the quantum vortices binding with the ith electron, which is displaced from the electron position $\langle\hat{\boldsymbol{\xi}}_i\rangle$ by a vector $-\boldsymbol{k}_i\times\hat{z}l_B^2$, according to the wave function Eq. (5).

We adopt $\{\boldsymbol{x}_i, \boldsymbol{p}_i \equiv \hbar\boldsymbol{k}_i\}$ as the set of dynamic variables, and interpret $\boldsymbol{x}_i$ and $\boldsymbol{p}_i$ as the position and momentum of a CP, respectively. To express the Lagrangian in $\{\boldsymbol{x}_i, \boldsymbol{p}_i\}$, it is necessary to relate the dynamic variables with the original set of parameters. From Eq. (5), it is easy to show that $\boldsymbol{x}_i$ is in general a function of $\{\boldsymbol{u}_i - \boldsymbol{k}_i\times\hat{z}l^2, i = 1\dots N\}$:

$$\boldsymbol{x}_i = \langle\hat{\boldsymbol{\xi}}_i\rangle_{\{\boldsymbol{k}_i=0, \boldsymbol{u}_i\to\boldsymbol{u}_i-\boldsymbol{k}_i\times\hat{z}l_B^2\}}, \tag{14}$$

where the expectation value is evaluated with respect to Eq. (5) with $\{\boldsymbol{k}_i = 0\}$ and substitutions $\{\boldsymbol{u}_i \to \boldsymbol{u}_i - \boldsymbol{k}_i\times\hat{z}l_B^2\}$. For a CPWC, we assume that both $\boldsymbol{x}_i$ and $\boldsymbol{p}_i$ are small, and adopt the harmonic approximation by expanding the Lagrangian to the second order of the dynamic variables. For this purpose, we expand $\boldsymbol{x}_i$ to the linear order of the original parameters:

$$x_{i\alpha} = \sum_{j\beta} A_{i\alpha,j\beta}(\boldsymbol{u}_j - \boldsymbol{k}_j\times\hat{z}l^2)_\beta, \tag{15}$$

and

$$A_{i\alpha,j\beta} \equiv \left.\frac{\partial\langle\hat{x}_{i\alpha}\rangle}{\partial u_{j\beta}}\right|_0 = \frac{1}{l_B^2}\langle\hat{\xi}_{i\alpha}\hat{\xi}_{j\beta}\rangle_0, \tag{16}$$

where $\alpha(\beta) = x, y$ indexes the component of the coordinate, $\langle\dots\rangle_0$ denotes the expectation value in the ground state $\Psi_0 \equiv \Psi|_{\{\boldsymbol{u}_i,\boldsymbol{k}_i\}\to 0}$, and $\epsilon_{\alpha\beta}$ is the two-dimensional Levi-Civita symbol.

Similarly, V_{ee} is expanded to the second order of the dynamic variables:

$$V_{ee} \approx \frac{1}{2}\sum_{i\alpha,j\beta} D^{\boldsymbol{xx}}_{i\alpha,j\beta}x_{i\alpha}x_{j\beta} + 2D^{\boldsymbol{px}}_{i\alpha,j\beta}p_{i\alpha}x_{j\beta} + D^{\boldsymbol{pp}}_{i\alpha,j\beta}p_{i\alpha}p_{j\beta}. \tag{17}$$

The coefficients can be related to correlation functions (see Appendix A):

$$D^{\boldsymbol{xx}}_{i\alpha,j\beta} = \frac{1}{l_B^4}\sum_{\gamma\delta}\langle(\hat{V}_{ee} - \bar{V}_{ee})\hat{\xi}_{l\gamma}\hat{\xi}_{m\delta}\rangle_0 \times [A^{-1}]_{i\alpha,l\gamma}[A^{-1}]_{m\delta,j\beta}, \tag{18}$$

$$D^{\boldsymbol{px}}_{i\alpha,j\beta} = -\frac{1}{\hbar}\sum_{\gamma\delta}\epsilon_{\alpha\gamma}\left\langle\frac{\partial\hat{V}_{ee}}{\partial r_{i\gamma}}\hat{\xi}_{l\delta}\right\rangle_0[A^{-1}]_{l\delta,j\beta}, \tag{19}$$

$$D^{\boldsymbol{pp}}_{i\alpha,j\beta} = \frac{l_B^4}{\hbar^2}\sum_{\gamma\delta}\epsilon_{\alpha\gamma}\epsilon_{\beta\delta}\left\langle\frac{\partial^2\hat{V}_{ee}}{\partial r_{i\gamma}\partial r_{j\delta}}\right\rangle_0, \tag{20}$$

where $[A^{-1}]$ denotes the inverse of a matrix with elements $[A]_{i\alpha,j\beta} = A_{i\alpha,j\beta}$, and $\bar{V}_{ee} \equiv \langle\hat{V}_{ee}\rangle_0$.

Substituting Eqs. (12), (13), (15), and (17) into Eq. (7), we determine the explicit form of the Lagrangian. Because of the translational symmetry, it is convenient to express the Lagrangian in the Fourier-transformed dynamic variables $\boldsymbol{x}(\boldsymbol{q}) \equiv 1/\sqrt{N}\sum_i \boldsymbol{x}_i\exp(-i\boldsymbol{q}\cdot\boldsymbol{R}_i^0)$ and $\boldsymbol{p}(\boldsymbol{q}) \equiv 1/\sqrt{N}\sum_i \boldsymbol{p}_i\exp(-i\boldsymbol{q}\cdot\boldsymbol{R}_i^0)$, where $\boldsymbol{q}$ is a wave vector defined in the Brillouin zone for a triangular lattice. The Lagrangian can be decomposed into $L = \sum_{\boldsymbol{q}} L_{\boldsymbol{q}}$ with

$$L_{\boldsymbol{q}} = \frac{eB_e(\boldsymbol{q})}{2}[\hat{z}\times\boldsymbol{x}^*(\boldsymbol{q})]\cdot\dot{\boldsymbol{x}}(\boldsymbol{q}) + \frac{1}{2eB}[\hat{z}\times\boldsymbol{p}^*(\boldsymbol{q})]\cdot\dot{\boldsymbol{p}}(\boldsymbol{q}) + \boldsymbol{p}^*(\boldsymbol{q})\cdot\dot{\boldsymbol{x}}(\boldsymbol{q}) - \frac{1}{2}\begin{bmatrix}\boldsymbol{x}(\boldsymbol{q})\\ \boldsymbol{p}(\boldsymbol{q})\end{bmatrix}^\dagger\mathcal{D}(\boldsymbol{q})\begin{bmatrix}\boldsymbol{x}(\boldsymbol{q})\\ \boldsymbol{p}(\boldsymbol{q})\end{bmatrix}, \tag{21}$$

where $B_e(\boldsymbol{q})$ is determined by

$$B_e(\boldsymbol{q}) = \frac{B}{2}\mathrm{Tr}\mathcal{A}^{-1}(\boldsymbol{q}), \tag{22}$$

with $\mathcal{A}^{-1}(\boldsymbol{q})$ being the inverse of a 2×2 matrix with elements $\mathcal{A}_{\alpha\beta}(\boldsymbol{q}) = \sum_{\boldsymbol{R}_i^0} A_{i\alpha,0\beta}\exp(-i\boldsymbol{q}\cdot\boldsymbol{R}_i^0)$, and

$$\mathcal{D}(\boldsymbol{q}) = \begin{bmatrix}\mathcal{D}^{\boldsymbol{xx}}(\boldsymbol{q}) & \mathcal{D}^{\boldsymbol{px}}(\boldsymbol{q})\\ \mathcal{D}^{\boldsymbol{px}}(\boldsymbol{q}) & \mathcal{D}^{\boldsymbol{pp}}(\boldsymbol{q})\end{bmatrix}, \tag{23}$$

with $\mathcal{D}^{\boldsymbol{xx}}(\boldsymbol{q})$, $\mathcal{D}^{\boldsymbol{px}}(\boldsymbol{q})$, and $\mathcal{D}^{\boldsymbol{pp}}(\boldsymbol{q})$ being the Fourier transforms of $D^{\boldsymbol{xx}}$, $D^{\boldsymbol{px}}$, and $D^{\boldsymbol{pp}}$, respectively.

The equation of motion of a type-I CPWC is

$$\begin{bmatrix}eB_e(\boldsymbol{q})\hat{z}\times & I\\ -I & \frac{1}{eB}\hat{z}\times\end{bmatrix}\begin{bmatrix}\dot{\boldsymbol{x}}(\boldsymbol{q})\\ \dot{\boldsymbol{p}}(\boldsymbol{q})\end{bmatrix} = -\mathcal{D}(\boldsymbol{q})\begin{bmatrix}\boldsymbol{x}(\boldsymbol{q})\\ \boldsymbol{p}(\boldsymbol{q})\end{bmatrix}, \tag{24}$$

which is the main result of this paper. The equation of motion can be written more generally as

$$\dot{\boldsymbol{x}}_i = \frac{\partial V_{ee}}{\partial\boldsymbol{p}_i} + \frac{1}{eB}\hat{z}\times\dot{\boldsymbol{p}}_i, \tag{25}$$

$$\dot{\boldsymbol{p}}_i = -\frac{\partial V_{ee}}{\partial\boldsymbol{x}_i} - \sum_j eB_e^{ij}\hat{z}\times\dot{\boldsymbol{x}}_j, \tag{26}$$

where $\mathcal{B}_e^{ij} = B\delta_{ij} - \Delta\mathcal{B}_e(\boldsymbol{R}_i^0 - \boldsymbol{R}_j^0)$ with $\Delta\mathcal{B}_e(\boldsymbol{R}^0) \equiv \int_{\rm BZ} d^2q/(2\pi)^2[B - B_e(\boldsymbol{q})]\exp(i\boldsymbol{q}\cdot\boldsymbol{R}^0)$. Interpretations of the dynamics and its implications to the nature of CPs will be discussed in Sec. III.

The equation of motion we obtain has a semiclassical form. One can always upgrade the dynamics to the quantum one by requantizing it. This can be done either by using path-integral formalism with the Lagrangian Eq. (21) or equivalently by applying a canonical quantization. On the other hand, under the harmonic approximation, we can show that results obtained from the semiclassical equation are identical to those obtained from a CF diagonalization. Both the points will be discussed in the next subsection.

C. Quantization of the effective dynamics

The dynamics Eq. (24) could be quantized. The resulting quantum dynamics describes the quantum evolution of the system in the submanifold of the Hilbert space specified by the wave function Eq. (5). A general scheme of the quantization has been discussed in Ref. [52]. Basically, the noncanonical kinematic matrix in the left-hand side of Eq. (24) gives rise to noncommutativity between the dynamic variables:

$$\begin{bmatrix} [\boldsymbol{x}^\dagger(\boldsymbol{q}),\boldsymbol{x}(\boldsymbol{q})] & [\boldsymbol{x}^\dagger(\boldsymbol{q}),\boldsymbol{p}(\boldsymbol{q})] \\ [\boldsymbol{p}^\dagger(\boldsymbol{q}),\boldsymbol{x}(\boldsymbol{q})] & [\boldsymbol{p}^\dagger(\boldsymbol{q}),\boldsymbol{p}(\boldsymbol{q})] \end{bmatrix} = i\hbar \begin{bmatrix} eB_e(\boldsymbol{q})\hat{\epsilon} & -I \\ I & \frac{1}{eB}\hat{\epsilon} \end{bmatrix}^{-1}, \tag{27}$$

where $\hat{\epsilon}$ is the 2×2 antisymmetric matrix with $[\hat{\epsilon}]_{\alpha\beta} = \epsilon_{\alpha\beta}$. The system is governed by an effective Hamiltonian $\hat{H}_{\rm eff} = V_{ee}$ with the dynamic variables upgraded to quantum operators.

The system can be transformed to a phonon representation by the procedure described in Ref. [43]. We solve the generalized eigenvalue equation:

$$i\omega_{\boldsymbol{q}} \begin{bmatrix} -eB_e(\boldsymbol{q})\hat{\epsilon} & I \\ -I & -\frac{1}{eB}\hat{\epsilon} \end{bmatrix} \psi_{\boldsymbol{q}} = \mathcal{D}(\boldsymbol{q})\psi_{\boldsymbol{q}}. \tag{28}$$

The equation yields two positive frequency solutions and two negative frequency solutions, with eigenvectors related by complex conjugations [43]. The eigenvectors are normalized by $\bar{\psi}_{\boldsymbol{q}}\psi_{\boldsymbol{q}} = \pm 1$, where $\pm$ is for the positive and the negative frequency solution, respectively, and

$$\bar{\psi}_{\boldsymbol{q}} \equiv -i\psi_{\boldsymbol{q}}^\dagger \begin{bmatrix} eB_e(\boldsymbol{q})\hat{\epsilon} & -I \\ I & \frac{1}{eB}\hat{\epsilon} \end{bmatrix}. \tag{29}$$

The dynamic variables can then be expressed in phonon creation and annihilation operators:

$$\begin{bmatrix} \boldsymbol{x}(\boldsymbol{q}) \\ \boldsymbol{p}(\boldsymbol{q}) \end{bmatrix} = \sum_{i\in+} \psi_{\boldsymbol{q}}^{(i)} a_{\boldsymbol{q}i} + \psi_{-\boldsymbol{q}}^{(i)*} a_{-\boldsymbol{q}i}^\dagger, \tag{30}$$

where the summation is over the two positive frequency solutions, and $a_{\boldsymbol{q}i}$ and $a_{\boldsymbol{q}i}^\dagger$ are bosonic creation and annihilation operators, respectively. One can verify that the dynamic variables, expressed as Eq. (30), do recover the commutation relation Eq. (27).

With the phonon representation, we define a coherent state as the eigenstate of the annihilation operator:

$$a_{\boldsymbol{q}i}|\phi\rangle = \phi_{\boldsymbol{q}i}|\phi\rangle. \tag{31}$$

In the real space, the coherent state is interpreted as

$$\langle \boldsymbol{r}|\phi\rangle = \frac{\Psi(\boldsymbol{r};\phi)}{\langle\Psi_0|\Psi\rangle}, \tag{32}$$

where the denominator is introduced to eliminate the time-dependent factor of the ground-state component in the wave function [49], and $\Psi(\boldsymbol{r};\phi)$ is the wave function Eq. (5) with the parameters corresponding to

$$\begin{bmatrix} \boldsymbol{x}^{(+)}(\boldsymbol{q}) \\ \boldsymbol{p}^{(+)}(\boldsymbol{q}) \end{bmatrix} = \sum_{i\in+} \psi_{\boldsymbol{q}}^{(i)} \phi_{\boldsymbol{q}i}, \tag{33}$$

where the superscript $(+)$ indicates that the dynamic variables contain positive-frequency components only [54].

For a given phonon state, the corresponding physical wave function can be determined by [54]

$$\langle \boldsymbol{r}|\varphi\rangle = \int \frac{d\phi d\phi^*}{2\pi i} e^{-|\phi|^2} \frac{\Psi(\boldsymbol{r};\phi)}{\langle\Psi_0|\Psi\rangle} \varphi(\phi^*), \tag{34}$$

where $\varphi(\phi^*)$ denotes a phonon wave function in the coherent-state representation. For the excited state with n phonons of the mode $(\boldsymbol{q},i)$, $\varphi(\phi^*) \propto \phi_{\boldsymbol{q}i}^{*n}$, the corresponding physical wave function is

$$\Psi_n(\boldsymbol{r}) \propto \frac{\partial^n}{\partial\phi_{\boldsymbol{q}i}^n} \frac{\Psi(\boldsymbol{r};\phi)}{\langle\Psi_0|\Psi\rangle}\bigg|_{\phi\to 0}. \tag{35}$$

From Eq. (35), it is easy to see that one-phonon states must be linear combinations of

$$\frac{\partial}{\partial\bar{u}_i}\frac{\Psi(\boldsymbol{r})}{\langle\Psi_0|\Psi\rangle}\bigg|_{\bar{u},k\to 0}, \quad \frac{\partial}{\partial k_i}\frac{\Psi(\boldsymbol{r})}{\langle\Psi_0|\Psi\rangle}\bigg|_{\bar{u},k\to 0}, \tag{36}$$

which correspond to many-body wave functions:

$$\hat{P}_{\rm LLL}(z_i - Z_i^0)\Psi_0, \quad \hat{P}_{\rm LLL}(\bar{z}_i - \bar{Z}_i^0)\Psi_0. \tag{37}$$

One can construct a CF diagonalization [1] by diagonalizing the microscopic Hamiltonian in the truncated Hilbert-space span by the bases Eq. (37). It is not difficult to see that its result will be identical to that obtained from the semiclassical equation of motion Eq. (24) [or equivalently Eq. (28)] under the harmonic approximation. This is because one could obtain a harmonic expansion of the Lagrangian Eq. (6) by expanding the trial wave function Eq. (5) to the linear order of $\{\boldsymbol{u}_i,\boldsymbol{k}_i\}$, i.e., as a linear combination of the bases Eq. (37). The eigenvalue equation of the CF diagonalization can be obtained from the time-dependent variational principle minimizing Eq. (6). Since the semiclassical dynamics are determined from the same variational principle, its result must be identical to that of the CF diagonalization.

However, there is still a subtle difference between the two approaches. This is because the harmonic expansion of Eq. (6) in the semiclassical approach requires expanding the trial wave function to the second order of $\{\boldsymbol{u}_i,\boldsymbol{k}_i\}$. It results in spurious terms not presented in the harmonic expansion for obtaining the CF diagonalization. In the next subsection, we will show that these terms are unphysical and can be eliminated by a projection.

D. Projected dynamic matrix

We note a subtlety concerning the quantum correspondence of the dynamics. In the derivation of the dynamics, we treat $\boldsymbol{x}_i$ and $\boldsymbol{p}_i$ as classical variables. However, when constructing the quantum coherent states, we use only the positive-frequency components of the dynamic variables, as shown in Eq. (33). The latter is necessary because the wave function $\langle \boldsymbol{r}|\phi\rangle$ defined in Eq. (32) should be the superposition of the ground state and excited states: $\langle \boldsymbol{r}|\phi\rangle \sim \Psi_0 + \sum_i \exp(-i\Delta E_i t)\Psi_i$ with $\Delta E_i > 0$, i.e., it only contains positive frequency components in its time dependence [54].

The consideration will introduce a modification to the harmonic expansion of V_{ee}. This is because the harmonic expansion Eq. (17), which treats the dynamic variable as classical variables, includes contributions from the second-order derivatives of the trial wave function with respect to $\{\boldsymbol{u}_i,\boldsymbol{k}_i\}$. These terms couple two positive- (negative-) frequency components of dynamic variables, and induce spurious couplings between positive- and negative-frequency branches in the resulting equation of motion. It is necessary to drop these terms in the harmonic expansion. On the other hand, one can show that the kinematic part of the dynamics is not affected by the issue.

To determine the modification, we note that our wave function Eq. (5) depends only on the complex variables $\bar{u}_i \equiv u_{xi} - iu_{yi}$ and $k_i \equiv k_{xi} + ik_{yi}$. Thus, $\bar{u}_i$ and k_i can be chosen to be positive-frequency functions of the time, and a proper harmonic expansion of V_{ee} should only include terms coupling $\{\bar{u}_i,k_i\}$ with their complex conjugates. To this end, we expand V_{ee} in terms of $\{\bar{\boldsymbol{u}}(\boldsymbol{q}),\boldsymbol{k}(\boldsymbol{q})\}$:

$$V_{ee} \approx \frac{1}{2}\sum_{\boldsymbol{q}} \begin{bmatrix} \boldsymbol{u}(\boldsymbol{q}) \\ \boldsymbol{k}(\boldsymbol{q}) \end{bmatrix}^{\dagger} \tilde{\mathcal{D}}(\boldsymbol{q}) \begin{bmatrix} \boldsymbol{u}(\boldsymbol{q}) \\ \boldsymbol{k}(\boldsymbol{q}) \end{bmatrix}, \tag{38}$$

where $\tilde{\mathcal{D}}(\boldsymbol{q})$ is the dynamic matrix with respect to $\{\boldsymbol{u}(\boldsymbol{q}),\boldsymbol{k}(\boldsymbol{q})\}$. To get rid of the spurious coupling, we introduce a projected dynamic matrix:

$$\tilde{\mathcal{D}}^P(\boldsymbol{q}) = \tilde{P}_+\tilde{\mathcal{D}}(\boldsymbol{q})\tilde{P}_+ + \tilde{P}_-^{\dagger}\tilde{\mathcal{D}}(\boldsymbol{q})\tilde{P}_-, \tag{39}$$

with

$$\tilde{P}_{\pm} = \begin{bmatrix} \frac{1}{2}(1\mp\sigma_2) & 0 \\ 0 & \frac{1}{2}(1\pm\sigma_2) \end{bmatrix}, \tag{40}$$

where σ_2 is the second Pauli matrix. The projection operators eliminate unwanted coupling in the original dynamic matrix $\tilde{\mathcal{D}}(\boldsymbol{q})$.

Similarly, we can obtain a projected dynamic matrix with respect to $\{\boldsymbol{x}(\boldsymbol{q}),\boldsymbol{p}(\boldsymbol{q})\}$ by a projection:

$$\mathcal{D}^P(\boldsymbol{q}) = P_+^{\dagger}(\boldsymbol{q})\mathcal{D}(\boldsymbol{q})P_+(\boldsymbol{q}) + P_-^{\dagger}(\boldsymbol{q})\mathcal{D}(\boldsymbol{q})P_-(\boldsymbol{q}), \tag{41}$$

with $P_{\pm} = U(\boldsymbol{q})\tilde{P}_{\pm}U^{-1}(\boldsymbol{q})$, where $U(\boldsymbol{q})$ is the transformation matrix relating $\{\bar{\boldsymbol{u}}(\boldsymbol{q}),\boldsymbol{k}(\boldsymbol{q})\}$ with $\{\boldsymbol{x}(\boldsymbol{q}),\boldsymbol{p}(\boldsymbol{q})\}$: $[\boldsymbol{x}(\boldsymbol{q}),\boldsymbol{p}(\boldsymbol{q})]^T = U(\boldsymbol{q})[\boldsymbol{u}(\boldsymbol{q}),\boldsymbol{k}(\boldsymbol{q})]^T$. We have

$$P_{\pm}(\boldsymbol{q}) = \begin{bmatrix} \frac{1}{2}\left(1\mp\mathcal{A}(\boldsymbol{q})\sigma_2\mathcal{A}^{-1}(\boldsymbol{q})\right) & \mp i\mathcal{A}(\boldsymbol{q}) \\ 0 & \frac{1}{2}(1\pm\sigma_2) \end{bmatrix}. \tag{42}$$

Substituting the dynamic matrix $\mathcal{D}(\boldsymbol{q})$ in Eqs. (24) and (28) with $\mathcal{D}^P(\boldsymbol{q})$, we eliminate the spurious couplings, and make the semiclassical approach completely equivalent to the CF diagonalization aforementioned [55].

III. INTERPRETATIONS OF THE CP DYNAMICS

A. Sundaram-Niu dynamics of CPs

The CP dynamics, as shown in Eq. (24), or Eqs. (25) and (26), is different from the one adopted in the heuristic approach, in which a CP is assumed to be an ordinary Newtonian particle characterized by an effective mass and a mean-field effective magnetic field [37–39]. Our CP dynamics fits in with the form of the more general Sundaram-Niu dynamics with Berry curvature corrections. An analysis of these corrections would provide insight into the nature of CPs, as we will discuss in the following.

First, CPs are subjected to an emergent gauge field $\Delta B_e(\boldsymbol{q}) \equiv B - B_e(\boldsymbol{q})$. The emergent gauge field gives rise to a dissipationless viscosity [43,44], resulting in the force characterized by $\mathcal{B}_e^{ij}$ shown in the right-hand side of Eq. (26). The presence of the emergent gauge field is actually anticipated in the conventional CF theory, in which it is manifested as Chern-Simons fields [40,56]. Specifically, the diagonal component of the emergent gauge field

$$\Delta B \equiv B - \mathcal{B}_e^{ii} = -\sum_{\boldsymbol{R}_i^0\neq 0} \Delta\mathcal{B}_e\left(\boldsymbol{R}_i^0\right) \tag{43}$$

corresponds to the Chern-Simons magnetic field, while the nondiagonal components induce a force in analogy to that induced by the Chern-Simons electric field resulting from moving quantum vortices through the Faraday effect [1]. However, in our formalism, the emergent gauge field in general cannot be described by the simple Chern-Simons action [57].

Second, CPs are subjected to a Berry curvature in the momentum space with $\Omega_z = 1/eB$ [58]. This is a feature of the dynamics not presented in the conventional theory of CFs [5,36]. The Berry curvature gives rise to an anomalous velocity, which is well known for electron dynamics in magnetic solids with spin-orbit coupling (SOC), and is linked to the (quantum) anomalous Hall effect [59,60]. Here, the Berry curvature is not induced by the SOC, but inherited from the Landau level hosting the particles. Indeed, a Landau level, when casted to a magnetic Bloch band, does have a uniformly distributed Berry curvature in the momentum space with $\Omega_z^{(\mathrm{LL})} = -1/eB$ [61]. One can show that the difference in the signs of Ω_z and $\Omega_z^{(\mathrm{LL})}$ is due to our assignment of the CP position to its constituent quantum vortices (see Sec. III C and Ref. [50]). The presence of a Berry curvature in the momentum space indicates that a CP is neither an ordinary Newtonian particle nor a Dirac particle, but a particle following the more general Sundaram-Niu dynamics.

B. Dipole interpretation

Our dynamics can be related to the dipole picture of CPs [36,47]. To see that, we interpret $\hat{z}\times\boldsymbol{p}_i/eB$ as the displacement from the electron to the quantum vortices bonded in a CP, and regard a CP as a dipole consisting of an electron and a bundle of m quantum vortices [36,47]. The picture and its relation to the usual position-momentum interpretation have

been discussed in Ref. [47]. For the interpretation, we adopt another set of dynamic variables:

$$\boldsymbol{x}_i^e = \langle \hat{\boldsymbol{r}}_i \rangle - \boldsymbol{R}_i^0 = \boldsymbol{x}_i - \frac{1}{eB}\hat{z} \times \boldsymbol{p}_i, \tag{44}$$

$$\boldsymbol{x}_i^\phi \equiv \boldsymbol{x}_i, \tag{45}$$

which are positions of the electron and the bundle of the quantum vortices, respectively. Note that the position of a CP is assigned to the position of the quantum vortices in Eq. (24).

The equation of motion with respect to the new dynamic variables is

$$\begin{bmatrix} e\Delta B_e(\boldsymbol{q})\hat{z}\times & 0 \\ 0 & -eB\hat{z}\times \end{bmatrix} \begin{bmatrix} \dot{\boldsymbol{x}}_\phi(\boldsymbol{q}) \\ \dot{\boldsymbol{x}}_e(\boldsymbol{q}) \end{bmatrix} = \mathcal{D}'(\boldsymbol{q}) \begin{bmatrix} \boldsymbol{x}_\phi(\boldsymbol{q}) \\ \boldsymbol{x}_e(\boldsymbol{q}) \end{bmatrix}, \tag{46}$$

where $\mathcal{D}'(\boldsymbol{q})$ is the corresponding dynamic matrix, which can be related to $\mathcal{D}^P(\boldsymbol{q})$ by a transformation.

It is notable from Eq. (46) that the electron in a CP is only coupled to the external magnetic field, while the quantum vortices are only coupled to the emergent gauge field [62]. Although not explicitly specified in the original proposal [47], the simple form of the coupling could have been anticipated from the microscopic wave function Eq. (5), in which the correlations introduced in the Bijl-Jastrow factor are between coordinates of quantum vortices. The particular way of the coupling should be regarded as an essential aspect of the dipole picture of CPs.

From Eq. (46), it also becomes apparent that our dynamics is consistent with Kohn's theorem. In the long-wavelength limit $\boldsymbol{q} \to 0$, both $\mathcal{D}'(\boldsymbol{q})$ and $\Delta B_e(\boldsymbol{q})$ vanish because of the translational symmetry. As a result, the degrees of freedom associating with $\boldsymbol{x}_\phi$ become degenerate. The system will only have a trivial zero-frequency mode, and no emergent mode will be present. The behavior is exactly what would be expected from Kohn's theorem, because the cyclotron mode, which is the only allowed resonance at $\boldsymbol{q} = 0$ according to the theorem, is an inter-Landau-level excitation, and will not appear in our dynamics, which has assumed that all excitations are within a Landau level.

From these observations, it becomes apparent that the presence of the Berry curvature in the momentum space would be an inevitable feature of the CP dynamics if we wanted to obtain the particular form of the dipole picture or conform to Kohn's theorem. Had we assumed a vanishing Berry curvature in Eq. (24), Eq. (46) would have a different form of the coupling to gauge fields, and its left-hand side would not become degenerate to conform to Kohn's theorem.

C. Definition of the CP position

In the position-momentum interpretation of the dynamics, there is arbitrariness in defining the position of a CP. In Eq. (24), the position of a CP is interpreted as the position of its constituent quantum vortices. It seems to be equally plausible to interpret the CP position as the electron position. Other choices are also possible. The issue is, will a different choice affect our interpretation of the dynamics?

To see that, we derive the equation of motion with respect to $\{\boldsymbol{x}_e(\boldsymbol{q}), \boldsymbol{p}(\boldsymbol{q})\}$. By substituting Eq. (44) into Eq. (24), it is straightforward to obtain

$$\begin{bmatrix} eB_e(\boldsymbol{q})\hat{z}\times & \frac{\Delta B_e(\boldsymbol{q})}{B} I \\ -\frac{\Delta B_e(\boldsymbol{q})}{B} I & -\frac{1}{eB}\left(\frac{\Delta B_e(\boldsymbol{q})}{B}\right)\hat{z}\times \end{bmatrix} \begin{bmatrix} \dot{\boldsymbol{x}}_e(\boldsymbol{q}) \\ \dot{\boldsymbol{p}}(\boldsymbol{q}) \end{bmatrix} = -\mathcal{D}''(\boldsymbol{q}) \begin{bmatrix} \boldsymbol{x}_e(\boldsymbol{q}) \\ \boldsymbol{p}(\boldsymbol{q}) \end{bmatrix}, \tag{47}$$

where $\mathcal{D}''(\boldsymbol{q})$ is the transformed dynamic matrix with respect to the new dynamic variables.

We observe that the equation of motion becomes more complicated. It still fits in with the general form of the Sundaram-Niu dynamics, but with a complicated structure of Berry curvatures [41]. Similar complexity also arises when one adopts other definitions of the CP position. The initial definition of the CP position stands out because it yields the simplest form of the dynamics.

On the other hand, the different choice of the CP position may have a physical consequence. This is the case when we apply an external electric field $\boldsymbol{E}$, which introduces a potential $\phi_{\text{ext}} = e\boldsymbol{E} \cdot \boldsymbol{x}_i^e = e\boldsymbol{E} \cdot (\boldsymbol{x}_i - \hat{z} \times \boldsymbol{p}_i/eB)$ into the system. We see that the CP carries an electric dipole $e\hat{z} \times \boldsymbol{p}_i/eB$ with respect to the external field if we adopt $\boldsymbol{x}_i$ as its position, while it is just a pure charge when the position of the CP is interpreted as $\boldsymbol{x}_i^e$. The different assignments of the position will affect how we define the equilibrium state of the system in the presence of an external electric field.

IV. NUMERICAL SIMULATIONS

A. Methods

We employ the Metropolis Monte-Carlo method to evaluate the coefficients defined in Eqs. (9) and (18)–(20). The algorithm and setup of our simulations are similar to those adopted in Ref. [8], with a couple of improvements detailed as follows.

First, our calculation employs a much larger simulation cell which involves 397 electrons arranged as 11 concentric hexagonal rings in a plane, as shown in the inset of Fig. 1. The larger simulation cell is needed to eliminate finite-size effects as the coefficients decay slowly in the real space.

Second, we use a different wave function for the finite simulation cell, and eliminate the need for introducing "ghost" particles explicitly. As pointed out in Ref. [8], in equilibrium ($\boldsymbol{R}_i = \boldsymbol{R}_i^0$, and $\boldsymbol{k}_i = 0$), the average positions of electrons do not coincide with their expected equilibrium positions due to the presence of the Bijl-Jastrow factor. As a result, it is necessary to introduce a cloud of ghost particles for each of the electrons. In Ref. [8], finite-size ghost-particle clouds were introduced. In our simulation, we extend the size of the ghost particle clouds to infinity. The resulting wave function can be determined analytically:

$$\Psi(\{\boldsymbol{r}_i\}) \propto \mathcal{A} \frac{\prod_{i<j\leqslant N} \left(z_i + ik_i l_B^2 - z_j - ik_j l_B^2\right)^m}{\prod_{i\leqslant N} \prod_{j\neq i,\leqslant N} \left(z_i + ik_j l_B^2 - Z_j^0\right)^m} \times \prod_{i=1}^{N} \left[\psi\left(z_i - Z_i^0 + ik_i l_B^2\right)\right]^m \phi_{\boldsymbol{R}_i}(\boldsymbol{r}_i), \tag{48}$$

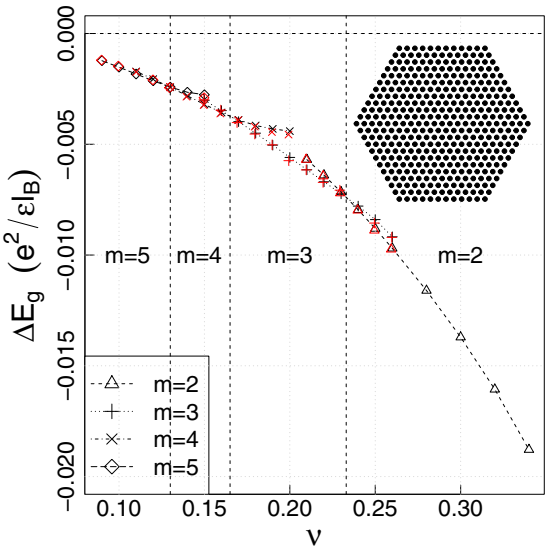

FIG. 1. Variational ground-state energies of CPWCs relative to that of the ordinary WC. Red points indicate the results of Ref. [8]. The phase boundaries between CPWC phases with different values of m are determined by comparing the energies, and indicated by dashed vertical lines. Inset: Configuration of the simulation cell.

where $Z_i^0 \equiv X_i^0 + iY_i^0$ [$\boldsymbol{R}_i^0 \equiv (X_i^0, Y_i^0)$], N is the total number of electrons in the simulation cell, and [37]

$$\psi(z) \equiv \frac{\prod_{i\neq 0}(z - Z_i^0)}{\prod_{i\neq 0}(Z_i^0)} \propto \frac{1}{z}\theta_1\left(\frac{z}{a}\middle|\frac{1}{2} + i\frac{\sqrt{3}}{2}\right), \tag{49}$$

where a is the lattice constant of the WC, the product is extended to an infinite triangular lattice with unit vectors $\boldsymbol{a}_1 = (1,0)a$ and $\boldsymbol{a}_2 = (1/2, \sqrt{3}/2)a$, and θ_1 is the Jacobi theta function.

An important issue of our simulation is to extrapolate the calculation results obtained in a finite simulation cell to the macroscopic limit. To this end, we find that A_0^{finite}, the coefficient defined in Eq. (16) calculated with a harmonic approximation of the wave function for the finite simulation cell [see Eq. (B3) in Appendix B], fits the long-range tail of the calculated coefficient very well. Hence, we divide the coefficient into a long-range part A_0^{finite} and a short-range part that decays rapidly with the distance, and fit the short-range part up to the fifth-nearest neighbors. The extrapolation is then straightforward by upgrading A_0^{finite} to its infinite lattice counterpart, which can be determined analytically.

Similar extrapolation schemes are applied for the determinations of the coefficients Eq. (18)–(20). We can have harmonic approximation for these coefficients as well [see Eq. (B5) in Appendix B]. They are regarded as the long-range parts of the coefficients. In this case, the remainder of the coefficients decays as $1/|\boldsymbol{R}_i^0 - \boldsymbol{R}_j^0|^5$ in the long range. We fit the remainders of $\mathcal{D}^{xx}$ and $\mathcal{D}^{px}$ with short-range terms up to the fifth-nearest neighbors, whereas for $\mathcal{D}^{pp}$ the higher precision of the calculated values allows us to fit it with a $1/|\boldsymbol{R}_i^0 - \boldsymbol{R}_j^0|^5$ term plus the short-range terms. We note that using the short-range terms to fit the remainders may yield an incorrect asymptotic behavior in the long-wavelength limit. It makes our determination of the dynamic matrix less reliable in the regime.

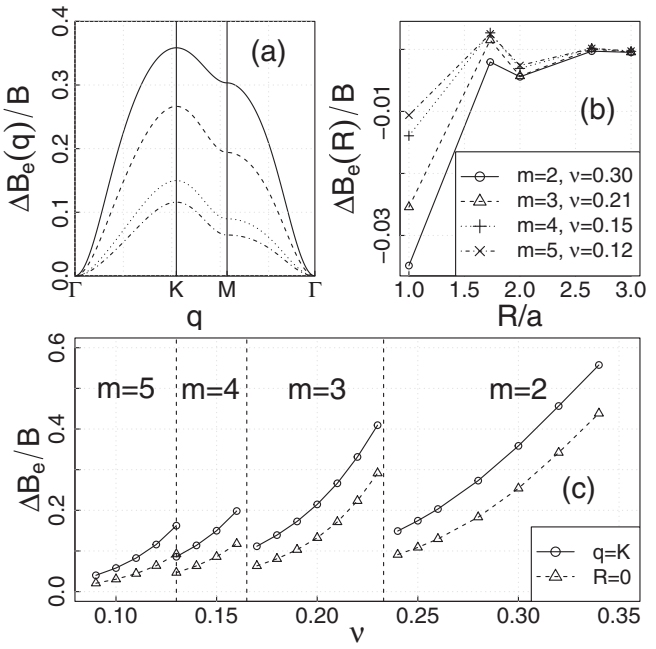

FIG. 2. Emergent gauge field. (a) Distribution of the emergent gauge field in the Brillouin zone for four representative filling factors [see legends in (b)] with different values of m. (b) Decay of the dissipationless viscosity coefficient $\Delta\mathcal{B}_e(\boldsymbol{R}_i^0)$ in the real space. R denotes the distance between two particles, and a is the lattice constant. (c) Filling factor ν dependence of the emergent gauge field at the K point of the Brillouin zone (circle-solid line) and the mean-field value ΔB defined in (43) (triangle-dashed line).

Figure 1 shows the variational ground-state energies determined from our simulations, and a comparison with the results presented in Ref. [8]. In our simulation, each of the Markov chains contains a total 5.6×10^{12} proposal states with an acceptance rate ∼25%. They yield essentially identical results as the old simulation (within the error bars of the old simulation) albeit with much improved precision.

B. Results

1. Emergent gauge field

Figure 2 shows the emergent gauge field ΔB_e. The distribution of the field in the Brillouin zone is shown in Fig. 2(a). It peaks at the K point and vanishes at the Γ point. In the real space, the dissipationless viscosity coefficient decays rapidly with the distance, as shown in Fig. 2(b).

The strength of the emergent gauge field is characterized either by the value of $\Delta B_e(\boldsymbol{q})$ at the K point or the mean-field value ΔB defined in Eq. (43). Both are shown in Fig. 2(c). The magnitude of the emergent field is ranged from a few percent to 10% of the external magnetic field, and is an increasing function of the filling factor for a given value of m. The magnitude is smaller than that expected for a FQH liquid, which has a mean-field value $\Delta B^{\text{FQH}}/B = m\nu$. It indicates the mean-field approximation adopted for FQH liquids is not applicable for the CPWCs. On the other hand, the magnitude

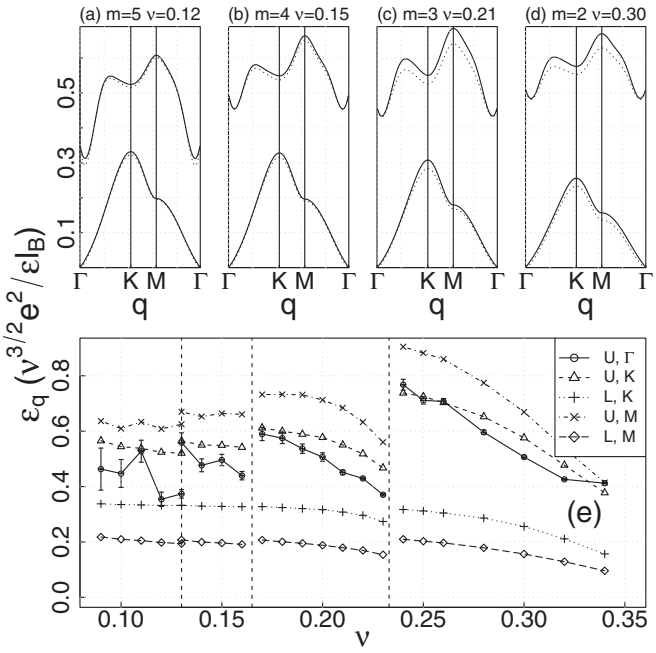

FIG. 3. Phonon dispersions of type-I CPWCs. (a–d) Phonon dispersions for a few representative filling factors. Both results using the projected dynamic matrix (solid lines) and the unprojected one (dotted lines) are shown. (e) Filling factor ν dependence of phonon energies of the upper (U) and the lower (L) branch at high-symmetry points of the Brillouin zone, including K point, M point, as well as Γ point (evaluated at $\boldsymbol{q} = 0.01\boldsymbol{K}$). $e^2/\epsilon l$ ($\approx 4.3\sqrt{B[\mathrm{T}]}$ meV for GaAs) is the Coulomb energy scale. Error bars for the phonon energies near the Γ point are shown.

is actually gigantic in comparison with that generated by an intrinsic SOC. For instance, the intrinsic SOC in GaAs could also give rise to a similar emergent gauge field in an ordinary 2D WC. However, its magnitude is of the order of $\sim$0.01 T only [63].

2. Phonon dispersions

The phonon dispersions of type-I CPWCs are obtained by solving the generalized eigenvalue equation Eq. (28). The results are summarized in Fig. 3. Among the two branches of phonons of a CPWC, the lower branch is not much different from that of an ordinary WC, both qualitatively and quantitatively [32–34], whereas the upper branch is an emergent mode with an energy scale $\sim 0.5\nu^{3/2}e^2/\epsilon l_B$, which is much smaller than the cyclotron energy. The upper branch has similar origin and energy scale as the magnetoroton mode arisen in FQH liquids [35]. We thus interpret the mode as the magnetoroton mode of the CPWC.

For typical experimental parameters, the energy of the emergent mode is much larger than the disorder pining modes which have been extensively probed by existing microwave experiments [16–24]. Our prediction thus calls for experiments probing into this energy regime.

3. Oscillator strength and Kohn's theorem

We also calculate the oscillator strength of the emergent magnetoroton mode. To do that, we determine the response

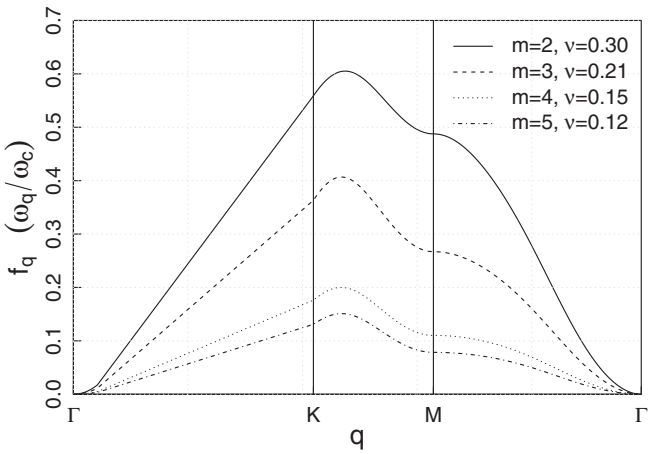

FIG. 4. Oscillator strength of the emergent magnetoroton mode for a few representative filling factors, in units of $\omega_{\boldsymbol{q}}/\omega_c$, where $\omega_{\boldsymbol{q}}$ is the frequency of the mode, and ω_c is the cyclotron frequency.

of the system to an external time-dependent electric field $\boldsymbol{E}(t) = \boldsymbol{E}_\omega \exp(-i\omega t)$. Because the external electric field is only coupled to the electron degree of freedom (see Sec. III B), it will introduce a scale potential $e\boldsymbol{E}(t)\cdot\boldsymbol{x}^e \equiv e\boldsymbol{E}(t)\cdot(\boldsymbol{x} - \hat{z}\times\boldsymbol{p}/eB)$ into the system. As a result, the equation of motion has the form

$$\begin{bmatrix} eB_e(\boldsymbol{q})\hat{z}\times & I \\ -I & \frac{1}{eB}\hat{z}\times \end{bmatrix}\begin{bmatrix} \dot{\boldsymbol{x}}(\boldsymbol{q}) \\ \dot{\boldsymbol{p}}(\boldsymbol{q}) \end{bmatrix} = -\mathcal{D}(\boldsymbol{q})\begin{bmatrix} \boldsymbol{x}(\boldsymbol{q}) \\ \boldsymbol{p}(\boldsymbol{q}) \end{bmatrix} + \begin{bmatrix} -e\boldsymbol{E}(t) \\ \boldsymbol{E}(t)\times\hat{z}/B \end{bmatrix}. \quad (50)$$

By solving the equation, we can determine the displacement of electrons parallel to the electric field, and the oscillator strength $f_{\boldsymbol{q}i}$ is defined by the relation [64] $x_e^{\parallel}(\boldsymbol{q}) = -e/m_b\sum_i f_{\boldsymbol{q}i}/(\omega_{\boldsymbol{q}i}^2 - \omega^2 - i\omega 0^+)E_\omega$, where m_b is the electron band mass of the 2DEG. The oscillator strength for the emergent magnetoroton mode is shown in Fig. 4. We see that it vanishes at the limit $\boldsymbol{q}\to 0$, in accordance with Kohn's theorem.

V. CONCLUDING REMARKS

In summary, we have derived the effective dynamics of CPs in a CPWC directly from its microscopic wave function. We find, most notably, the presence of a Berry curvature in the momentum space. The picture emerged from the dynamics is different from the conventional one that assumes that a CP behaves just like an ordinary Newtonian particle. On the other hand, we show that the dynamics is consistent with the dipole picture of CPs, and the presence of the Berry curvature is actually an inevitable consequence of the picture. The consistency is not a coincidence, since both are derived from microscopic wave functions. The discrepancy between our picture and the conventional interpretation of CPs is not surprising because the conventional picture was developed from a flux-attachment argument for free particles residing in a parabolic band [40], while ours is constructed for electrons constrained in a Landau level. The Berry curvature is just a result of the projection to the Landau level.

The equations of motion Eqs. (25) and (26), which are derived for type-I CPWCs, can be generalized for general CP systems by interpreting $\mathcal{B}_e^{ij}$ as a function of $\{\boldsymbol{x}_i\}$ and the effective CP Hamiltonian V_{ee} as a function of $\{\boldsymbol{x}_i, \boldsymbol{p}_i\}$ [65]. This is possible because all CP wave functions with the form of Eq. (1) can be expanded as linear combinations of the set of wave functions specified by Eq. (5) with different parameters $\{\boldsymbol{R}_i, \boldsymbol{k}_i\}$, which could be regarded as "coherent-state" bases of CPs. Hence, Eqs. (25) and (26) could be regarded as the equations of motion with respect to coherent-state coordinates and momenta. The key insight obtained in this paper, i.e., the presence of a Berry curvature in the momentum space, will carry over into the general CP dynamics. The correction introduced by the Berry curvature would be sufficient to cure the deficiencies of the conventional CF theory noted in Ref. [45]: (a) the anomalous Hall effect induced by the Berry curvature yields a nonvanishing Hall conductance of CFs in a half-filled Landau level, and (b) the density-of-state correction associating with the Berry curvature induces the apparent asymmetry in the CF pictures for a filling fraction and its hole conjugate. A tentative CP theory taking account of the Berry curvature correction is presented in Ref. [50].

ACKNOWLEDGMENTS

This paper is supported by National Basic Research Program of China (973 Program) Grant No. 2015CB921101 and National Natural Science Foundation of China Grant No. 11325416.

APPENDIX A: DYNAMIC MATRIX

To derive the formulas for the dynamic matrix coefficients (18)–(20), we make use of the identities

$$\frac{\partial V_{ee}}{\partial x_{i\alpha}} = \frac{\partial V_{ee}}{\partial u_{j\beta}}[A^{-1}]_{j\beta,i\alpha}, \tag{A1}$$

$$\frac{\partial V_{ee}}{\partial p_{i\alpha}} = \frac{1}{\hbar}\left(\frac{\partial}{\partial k_{i\alpha}} - l_B^2\epsilon_{\alpha\beta}\frac{\partial}{\partial u_{i\beta}}\right)V_{ee}, \tag{A2}$$

$$\frac{\partial|\Psi|^2}{\partial u_{i\alpha}} = \frac{r_{i\alpha} - R_{i\alpha}}{l_B^2}|\Psi|^2, \tag{A3}$$

$$\frac{\partial|\Psi|^2}{\partial p_{i\alpha}} = \tfrac{1}{\hbar}\left(\tfrac{\partial}{\partial k_{i\alpha}} - l_B^2\epsilon_{\alpha\beta}\tfrac{\partial}{\partial u_{i\beta}}\right)|\Psi|^2 = \tfrac{l_B^2}{\hbar}\epsilon_{\alpha\beta}\tfrac{\partial|\Psi|^2}{\partial r_{i\beta}}. \tag{A4}$$

In deriving the last identity, we make use of Eq. (10). We obtain

$$\frac{\partial V_{ee}}{\partial x_{i\alpha}} = \frac{1}{l_B^2}\langle(\hat{V}_{ee} - \bar{V}_{ee})(\hat{r}_{j\beta} - R_{j\beta})\rangle[A^{-1}]_{j\beta,i\alpha}, \tag{A5}$$

$$\frac{\partial V_{ee}}{\partial p_{i\alpha}} = -\frac{l_B^2}{\hbar}\epsilon_{\alpha\beta}\left\langle\frac{\partial \hat{V}_{ee}}{\partial r_{i\beta}}\right\rangle. \tag{A6}$$

Applying the second derivative, and making use the identities again, we obtain Eqs. (18)–(20).

APPENDIX B: HARMONIC APPROXIMATIONS OF THE COEFFICIENTS

A rudimentary approximation for evaluating the coefficients is the harmonic approximation. We define the harmonic approximation of the wave function as

$$|\Psi_0|^2 \propto \exp\left[2m\sum_{i<j}\ln|\boldsymbol{r}_i - \boldsymbol{r}_j|^2 - \frac{1}{2l_B^2}\sum_i|\boldsymbol{r}_i - \boldsymbol{R}_i^0|^2\right]$$

$$\approx \exp\left[-\frac{1}{2}\sum_{ij,\alpha\beta}F_{\alpha\beta}\left(\boldsymbol{R}_i^0 - \boldsymbol{R}_j^0\right)\xi_{i\alpha}\xi_{j\beta}\right], \tag{B1}$$

where

$$F_{\alpha\beta}\left(\boldsymbol{R}_i^0\right) = \begin{cases}\frac{1}{l_B^2}\delta_{\alpha\beta} & \boldsymbol{R}_i^0 = 0\\ -2m\frac{2R_{i\alpha}^0R_{i\beta}^0 - |\boldsymbol{R}_i^0|^2\delta_{\alpha\beta}}{|\boldsymbol{R}_i^0|^4} & \boldsymbol{R}_i^0 \neq 0\end{cases}. \tag{B2}$$

Under the approximation, the coefficient A defined in Eq. (16) is related to F by a matrix inversion:

$$A \approx A_0 \equiv \frac{1}{l_B^2}F^{-1}. \tag{B3}$$

The coefficient $F_{\alpha\beta}(\boldsymbol{R}_i^0)$ satisfies an identity:

$$\sum_\alpha F_{\alpha\alpha}\left(\boldsymbol{R}_i^0\right) = \frac{2}{l_B^2}\delta_{\boldsymbol{R}_i^0,0}. \tag{B4}$$

It leads to a vanishing emergent gauge field.

To evaluate the dynamic matrix, we first expand the electron-electron interaction operator $\hat{V}_{ee}$ to the second order of $\hat{\boldsymbol{\xi}}_i$. With the approximated wave function Eq. (B1), the coefficients (18)–(20) become Gaussian integrals. We obtain the harmonic approximation of the dynamic matrix:

$$\mathcal{D}_0(\boldsymbol{q}) = \begin{bmatrix} D_0(\boldsymbol{q}) & \frac{l_B^2}{\hbar}D_0(\boldsymbol{q})\hat{\epsilon} \\ -\frac{l_B^2}{\hbar}\hat{\epsilon}D_0(\boldsymbol{q}) & -\frac{l_B^4}{\hbar^2}\hat{\epsilon}D_0(\boldsymbol{q})\hat{\epsilon}\end{bmatrix}, \tag{B5}$$

where $D_0(\boldsymbol{q})$ is the 2×2 classical dynamic matrix of the WC.

[1] J. K. Jain, *Composite Fermions* (Cambridge University, Cambridge, England, 2007).
[2] J. K. Jain and P. W. Anderson, Beyond the fermi liquid paradigm: Hidden fermi liquids, Proc. Natl. Acad. Sci. USA **106**, 9131 (2009).
[3] O. Heinonen, *Composite Fermions: A Unified View of the Quantum Hall Regime* (World Scientific, Singapore, 1997).
[4] V. Kalmeyer and S.-C. Zhang, Metallic phase of the quantum Hall system at even-denominator filling fractions, Phys. Rev. B **46**, 9889 (1992).
[5] B. I. Halperin, P. A. Lee, and N. Read, Theory of the half-filled Landau level, Phys. Rev. B **47**, 7312 (1993).
[6] G. Moore and N. Read, Nonabelions in the fractional quantum Hall effect, Nucl. Phys. B **360**, 362 (1991).

[7] G. Giuliani and G. Vignale, *Quantum Theory of the Electron Liquid* (Cambridge University, Cambridge, England, 2005).

[8] H. Yi and H. A. Fertig, Laughlin-Jastrow-correlated Wigner crystal in a strong magnetic field, Phys. Rev. B **58**, 4019 (1998).

[9] R. Narevich, G. Murthy, and H. A. Fertig, Hamiltonian theory of the composite-fermion Wigner crystal, Phys. Rev. B **64**, 245326 (2001).

[10] A. C. Archer, K. Park, and J. K. Jain, Competing Crystal Phases in the Lowest Landau Level, Phys. Rev. Lett. **111**, 146804 (2013).

[11] K. Yang, F. D. M. Haldane, and E. H. Rezayi, Wigner crystals in the lowest Landau level at low-filling factors, Phys. Rev. B **64**, 081301 (2001).

[12] S.-Y. Lee, V. W. Scarola, and J. K. Jain, Structures for interacting composite fermions: Stripes, bubbles, and fractional quantum Hall effect, Phys. Rev. B **66**, 085336 (2002).

[13] M. O. Goerbig, P. Lederer, and C. M. Smith, Possible Reentrance of the Fractional Quantum Hall Effect in the Lowest Landau Level, Phys. Rev. Lett. **93**, 216802 (2004).

[14] C.-C. Chang, G. S. Jeon, and J. K. Jain, Microscopic Verification of Topological Electron-Vortex Binding in the Lowest Landau-Level Crystal State, Phys. Rev. Lett. **94**, 016809 (2005).

[15] C.-C. Chang, C. Töke, G. S. Jeon, and J. K. Jain, Competition between composite-fermion-crystal and liquid orders at $\nu = 1/5$, Phys. Rev. B **73**, 155323 (2006).

[16] E. Y. Andrei, G. Deville, D. C. Glattli, F. I. B. Williams, E. Paris, and B. Etienne, Observation of a Magnetically Induced Wigner Solid, Phys. Rev. Lett. **60**, 2765 (1988).

[17] L. W. Engel, C. C. Li, D. Shahar, D. C. Tsui, and M. Shayegan, Microwave resonances in low-filling insulating phases of two-dimensional electron and hole systems, Physica E **1**, 111 (1997).

[18] C.-C. Li, L. W. Engel, D. Shahar, D. C. Tsui, and M. Shayegan, Microwave Conductivity Resonance of Two-Dimensional Hole System, Phys. Rev. Lett. **79**, 1353 (1997).

[19] C.-C. Li, J. Yoon, L. W. Engel, D. Shahar, D. C. Tsui, and M. Shayegan, Microwave resonance and weak pinning in two-dimensional hole systems at high magnetic fields, Phys. Rev. B **61**, 10905 (2000).

[20] Y. P. Chen, R. M. Lewis, L. W. Engel, D. C. Tsui, P. D. Ye, L. N. Pfeiffer, and K. W. West, Microwave Resonance of the 2D Wigner Crystal around Integer Landau Fillings, Phys. Rev. Lett. **91**, 016801 (2003).

[21] Y. P. Chen, R. M. Lewis, L. W. Engel, D. C. Tsui, P. D. Ye, Z. H. Wang, L. N. Pfeiffer, and K. W. West, Evidence for Two Different Solid Phases of Two-Dimensional Electrons in High Magnetic Fields, Phys. Rev. Lett. **93**, 206805 (2004).

[22] Y. P. Chen, G. Sambandamurthy, Z. H. Wang, R. M. Lewis, L. W. Engel, D. C. Tsui, P. D. Ye, L. N. Pfeiffer, and K. W. West, Melting of a 2D quantum electron solid in high magnetic field, Nat. Phys. **2**, 452 (2006).

[23] H. Zhu, Y. P. Chen, P. Jiang, L. W. Engel, D. C. Tsui, L. N. Pfeiffer, and K. W. West, Observation of a Pinning Mode in a Wigner Solid with $\nu = 1/3$ Fractional Quantum Hall Excitations, Phys. Rev. Lett. **105**, 126803 (2010).

[24] F. I. B. Williams, P. A. Wright, R. G. Clark, E. Y. Andrei, G. Deville, D. C. Glattli, O. Probst, B. Etienne, C. Dorin, C. T. Foxon, and J. J. Harris, Conduction Threshold and Pinning Frequency of Magnetically Induced Wigner Solid, Phys. Rev. Lett. **66**, 3285 (1991).

[25] C. Zhang, R.-R. Du, M. J. Manfra, L. N. Pfeiffer, and K. W. West, Transport of a sliding Wigner crystal in the four flux composite fermion regime, Phys. Rev. B **92**, 075434 (2015).

[26] Y. Liu, D. Kamburov, S. Hasdemir, M. Shayegan, L. N. Pfeiffer, K. W. West, and K. W. Baldwin, Fractional Quantum Hall Effect and Wigner Crystal of Interacting Composite Fermions, Phys. Rev. Lett. **113**, 246803 (2014).

[27] W. Pan, H. L. Stormer, D. C. Tsui, L. N. Pfeiffer, K. W. Baldwin, and K. W. West, Transition from an Electron Solid to the Sequence of Fractional Quantum Hall States at Very Low Landau Level Filling Factor, Phys. Rev. Lett. **88**, 176802 (2002).

[28] Y. P. Li, T. Sajoto, L. W. Engel, D. C. Tsui, and M. Shayegan, Low-Frequency Noise in the Reentrant Insulating Phase Around the 1/5 Fractional Quantum Hall Liquid, Phys. Rev. Lett. **67**, 1630 (1991).

[29] H. W. Jiang, H. L. Stormer, D. C. Tsui, L. N. Pfeiffer, and K. W. West, Magnetotransport studies of the insulating phase around $\nu = 1/5$ Landau-level filling, Phys. Rev. B **44**, 8107 (1991).

[30] H. W. Jiang, R. L. Willett, H. L. Stormer, D. C. Tsui, L. N. Pfeiffer, and K. W. West, Quantum Liquid Versus Electron Solid Around $\nu = 1/5$ Landau-Level Filling, Phys. Rev. Lett. **65**, 633 (1990).

[31] V. J. Goldman, M. Santos, M. Shayegan, and J. E. Cunningham, Evidence for Two-Dimensional Quantum Wigner Crystal, Phys. Rev. Lett. **65**, 2189 (1990).

[32] K. Maki and X. Zotos, Static and dynamic properties of a two-dimensional Wigner crystal in a strong magnetic field, Phys. Rev. B **28**, 4349 (1983).

[33] R. Côté and A. H. MacDonald, Phonons as Collective Modes: The Case of a Two-Dimensional Wigner Crystal in a Strong Magnetic Field, Phys. Rev. Lett. **65**, 2662 (1990).

[34] R. Côté and A. H. MacDonald, Collective modes of the two-dimensional Wigner crystal in a strong magnetic field, Phys. Rev. B **44**, 8759 (1991).

[35] S. M. Girvin, A. H. MacDonald, and P. M. Platzman, Magneto-roton theory of collective excitations in the fractional quantum Hall effect, Phys. Rev. B **33**, 2481 (1986).

[36] S. H. Simon, The Chern-Simons Fermi Liquid Description of Fractional Quantum Hall States, in *Composite Fermions* (World Scientific, Singapore, 1998), pp. 91–194.

[37] J.-W. Rhim, J. K. Jain, and K. Park, Analytical theory of strongly correlated Wigner crystals in the lowest Landau level, Phys. Rev. B **92**, 121103 (2015).

[38] A. C. Archer and J. K. Jain, Static and dynamic properties of type-II composite fermion Wigner crystals, Phys. Rev. B **84**, 115139 (2011).

[39] A. M. Ettouhami, F. D. Klironomos, and A. T. Dorsey, Static and dynamic properties of crystalline phases of two-dimensional electrons in a strong magnetic field, Phys. Rev. B **73**, 165324 (2006).

[40] A. Lopez and E. Fradkin, Fractional quantum Hall effect and Chern-Simons gauge theories, Phys. Rev. B **44**, 5246 (1991).

[41] G. Sundaram and Q. Niu, Wave-packet dynamics in slowly perturbed crystals: Gradient corrections and Berry-phase effects, Phys. Rev. B **59**, 14915 (1999).

[42] D. Xiao, M.-C. Chang, and Q. Niu, Berry phase effects on electronic properties, Rev. Mod. Phys. **82**, 1959 (2010).

[43] T. Qin, J. Zhou, and J. Shi, Berry curvature and the phonon Hall effect, Phys. Rev. B **86**, 104305 (2012).

[44] T. L. Hughes, R. G. Leigh, and E. Fradkin, Torsional Response and Dissipationless Viscosity in Topological Insulators, Phys. Rev. Lett. **107**, 075502 (2011).

[45] D. T. Son, Is the Composite Fermion a Dirac Particle? Phys. Rev. X **5**, 031027 (2015).

[46] D. T. Son, The Dirac composite fermion of the fractional quantum Hall effect, Prog. Theor. Exp. Phys. **2016**, 12C103 (2016).

[47] N. Read, Theory of the half-filled Landau level, Semicond. Sci. Technol. **9**, 1859 (1994).

[48] E. Rezayi and N. Read, Fermi-Liquid-Like State in a Half-Filled Landau Level, Phys. Rev. Lett. **72**, 900 (1994).

[49] P. Kramer and M. Saraceno, *Geometry of the Time-Dependent Variational Principle in Quantum Mechanics* (Springer, New York, 1981).

[50] J. Shi, Chern-simons theory and dynamics of composite fermions, arXiv:1704.07712 (2017).

[51] We have assumed that the direction of $q\boldsymbol{B}$ is along $+\hat{z}$ direction, where q is the charge of a carrier, and $\hat{z}$ is the normal direction of the 2DEG plane. For the opposite case, one should define $z_i = x_i - iy_i$ instead.

[52] D. Xiao, J. Shi, and Q. Niu, Berry Phase Correction to Electron Density of States in Solids, Phys. Rev. Lett. **95**, 137204 (2005).

[53] We should interpret $\boldsymbol{R}_i^0$ here as the averaged position $\langle \boldsymbol{r}_i \rangle_0$. It is assumed to be coinciding with $\boldsymbol{R}_i^0$ appearing in Eq. (3). However, this is in general not true for the reason discussed in Sec. IV A, where a remedy is also presented. A more straightforward solution would just treat $\boldsymbol{R}_i^0$ appearing in Eq. (3) as a (variational) parameter, and adjust its value so that $\langle \boldsymbol{r}_i \rangle_0$ coincides with its expected position in the triangular lattice. In any case, it is simply a reparametrization and will not affect our result.

[54] R. J. Glauber, Coherent and incoherent states of the radiation field, Phys. Rev. **131**, 2766 (1963).

[55] There is still a minor difference: the semiclassical approach contains both the positive and negative frequency branches. This is needed for a classical interpretation. The two branches are decoupled in the eigenvalue equation with the projected dynamic matrix, and the CF diagonalization is the positive frequency half.

[56] S. C. Zhang, The Chern-Simons-Landau-Ginzburg theory of the fractional quantum Hall effect, Int. J. Mod. Phys. B **06**, 25 (1992).

[57] One can show that the vector potential experienced by a CP is $\boldsymbol{A}_{x_i} = (eB/2)\hat{z} \times (\boldsymbol{R}_i - \boldsymbol{k}_i \times \hat{z} l_B^2) = (eB/2)\hat{z} \times \boldsymbol{x}_i - m\hbar \langle \sum_{j \neq i} \hat{z} \times (\hat{\boldsymbol{r}}_i - \hat{\boldsymbol{r}}_j)/|\hat{\boldsymbol{r}}_i - \hat{\boldsymbol{r}}_j|^2 \rangle_0'$, where $\langle \ldots \rangle_0'$ denotes the expectation value in the wave function Eq. (5) with $\{\boldsymbol{k}_i = 0, i = 1 \ldots N\}$, and the remaining parameters of the wave function are set implicitly by the condition $\langle \hat{\boldsymbol{r}}_i - \boldsymbol{R}_i^0 \rangle_0' = \boldsymbol{x}_i$. While the formula looks similar to its counterpart in the Chern-Simons theory [1,56], it has an important difference: the dynamic valuables are $\{\boldsymbol{x}_i\}$ instead of $\{\hat{\boldsymbol{r}}_i\}$.

[58] Because of the general relation Eq. (14), we can show that the Berry curvature $\Omega_z = 1/eB$ is valid for arbitrary $\{\boldsymbol{x}_i, \boldsymbol{p}_i\}$, not limited to small amplitudes as implied by the harmonic approximation.

[59] T. Jungwirth, Q. Niu, and A. H. MacDonald, Anomalous Hall Effect in Ferromagnetic Semiconductors, Phys. Rev. Lett. **88**, 207208 (2002).

[60] F. D. M. Haldane, Model for a Quantum Hall Effect without Landau Levels: Condensed-Matter Realization of the "Parity Anomaly," Phys. Rev. Lett. **61**, 2015 (1988).

[61] Y. Zhang and J. Shi, Mapping a fractional quantum Hall state to a fractional Chern insulator, Phys. Rev. B **93**, 165129 (2016).

[62] A. C. Potter, M. Serbyn, and A. Vishwanath, Thermoelectric Transport Signatures of Dirac Composite Fermions in the Half-Filled Landau Level, Phys. Rev. X **6**, 031026 (2016).

[63] W.-C. Ji and J.-R. Shi, Topological phonon modes in a two-dimensional wigner crystal, Chin. Phys. Lett. **34**, 036301 (2017).

[64] J. D. Jackson, *Classical Electrodynamics* (Wiley, New York, 1999).

[65] The emergent gauge field will have extra components when the density distribution of CPs breaks the inversion symmetry. This will be presented elsewhere.